ORIGINAL PAPER

Preparation and characterization of powdered and granular activated carbon from Palmae biomass for cadmium removal

D. E. Egirani[1] **· N. R. Poyi**[2] **· N. Shehata**[3]

Abstract

This paper investigated the characteristics of powdered activated carbon (PAC) and granular activated carbon (GAC) derived from African Palmae shell and its application in the removal of cadmium(II) ions in aqueous media. The African Palmae shell is obtained from a widely and easily grown palm tree found in the African tropics. This biomass has not been adequately studied as a precursor in the production of activated carbon. Palmae shell has been processed into powdered and activated carbon and tested for its efficiency in removing cadmium(II) (Cd(II)) ions. The characterization includes determination of proximate analysis, ultimate analysis, point of zero charges, and surface area. The reaction mechanism and kinetics were predicated on the proton coefficient that was < 1 for both PAC and GAC, some mass transfer rates, and intraparticle diffusion. The values for these characteristics revealed that protonation was not actively involved in the adsorption process. The reaction also was not a rate-limiting process. The parametric batch mode studies of contact time (maximizing at 93.2% for PAC and 83.5% for GAC), initial Cd(II) concentration, pH (93% for PAC and 88% for GAC), and dosage of activated carbon indicated that PAC readily removes Cd(II) than GAC. Both PAC and GAC derived from Palmae shell are, therefore, novel biosorbents.

Keywords Preparation · Characterization · Powdered activated carbon · Granular activated carbon · Cadmium removal · Palmae biomass

Introduction

An aggregation of toxic heavy metals such as cadmium, above international recommended limits, poses a grave danger to human health and the ecosystem. The biggest recipient of these metals is the aquatic environment. These toxic heavy metals include arsenic, mercury, lead, cadmium among others. Several sources of toxic heavy metals have been identified (Šapčanin et al. 2019). These sources include extraction of ores, refining of ores, industrial application of these toxic heavy metals, urban waste, and agricultural waste (Sierra-Marquez et al. 2019). One of the toxic heavy metals of interest is cadmium (Cd). The presence of cadmium above recommended limits of 0.003 mg L^{-1} in the aquatic environment has generated lots of scientific interest. This interest is predicated on the fact that cadmium is a carcinogenic element (Shahraki et al. 2018). An assembly of Cd discharged into the aquatic environment could lead to contamination of the food chain, and subsequent deposition of this toxic element in the vital organs of human. Human liver and kidney become dysfunctional due to the development of stalled calcium metabolism, skeleton damage, and kidney stones (Zhang and Reynolds 2019).

Several treatment techniques have been adopted in the past for the removal of Cd from aqueous media (Barsbay et al. 2018). These techniques include the use of filters, use of oxidizing agents, sediment settling, a distillation of the affected aqueous system, use of osmosis in reverse order, use of electrodes in chemical processing, and use of ion exchangers (Imran et al. 2019). The chemical precipitation technique and regeneration of adsorbents by electrochemical method do not achieve an international recommended limit of the low concentration of toxic heavy metal ions in aqueous media. In some cases, a large volume of sludge

---

✉ D. E. Egirani
    eenonidavidson@yahoo.com; enopmc@enopmcservices.com

1   Faculty of Science, Niger Delta University,
    Wilberforce Island, Nigeria

2   Nigerian Institute of Mining and Geosciences, Jos, Nigeria

3   Faculty of the Postgraduates Studies for Advanced Sciences,
    Beni-Suef University, Beni Suef, Egypt

is produced and this large volume is difficult to treat. Ion exchange and membrane filtration techniques are excellent methods of handling toxic heavy metals in wastewater (Egirani et al. 2019). Some of these techniques are, however, expensive and undesirable in treating large volume of wastewater. Some of these techniques also are unable to provide acceptable outcomes in a large-scale wastewater treatment process. The adsorption technique, however, has been considered as one of the best treatment techniques because this process is simple in design, easy to operate, and environmentally friendly if biosorbents are used (Wang et al. 2019).

In adsorption, molecules of adsorbate are attached from a solution onto the surface of an adsorbent by forces of attraction. The adsorption technique, using activated carbon, is one of the ways to eliminate this problem of Cd in aqueous system. Activated carbon is a highly carbonaceous, porous, and adsorptive medium with a complex structure consisting essentially of carbon atoms. Activated carbon is produced from various types of biomaterials. Some of these biomasses are cheaper and some are expensive (Thambiliyagodage et al. 2018). Ordinarily, the cultivation of these biomaterials adds to the cost of production. There is a need, therefore, to source for a biomass that is wildly and easily grown in proximity to a place of use. A low-cost production strategy is needed without compromising the efficiency of some adsorption properties of activated carbon (Sadegh et al. 2017). Some properties of activated carbon also required for efficient performance as biosorbents include the nature of the activator and the physical properties of the activated carbon. The chemical activation process involves the impregnation of the biomass as a precursor with certain chemicals at a defined ratio. Subsequently, the impregnated biomass is carbonized at a lower temperature when compared with physical activation. In physical activation, the biomass is pyrolysed at a higher temperature when compared with chemical activation (Janković et al. 2019). Pyrolysis is conducted under inert gas flow condition. Subsequently, the carbonized biomass is subjected to oxidation at a very high temperature and pressure. The chemical activation process is preferred over a physical activation because this process is low temperature and shorter time-dependent (Di Stasi et al. 2019). A higher exposed surface also is provided by this process when compared with the physical activation process. The chemical modification process for activated carbon also provides more adsorption sites for the activated carbon surface (Yin et al. 2018). Some chemicals normally employed in the activation process include zinc chloride ($ZnCl_2$), phosphoric acid (H_3PO_4), sulphuric acid (H_2SO_4), potassium hydroxide (KOH), and sodium hydroxide (NaOH). The use of hydroxides, however, provides additional hydroxyl reactive sites for activated carbon. Thus, the use of KOH is preferable because KOH as an activator provides a high surface area and highly microporous characteristics (Yacob

et al. 2010). The chemical activation process consists of both direct and char activation techniques. In the direct chemical activation, the precursor is dried, chemically treated, and dried in a muffle furnace between 400 and 700 °C. In char-impregnated chemical activation, a char is impregnated with an activator and subsequently heated in a muffle furnace at the required temperature between 400 and 700 °C. The latter treatment is recognized as a better procedure because the textural property of the activated carbon is enhanced (Yang et al. 2019). The choice of powered or granular activated carbon is dependent on the purposes of production of the activated carbon. Powdered activated carbon, however, possesses a higher exposed surface area when compared with granular activated carbon (Wan Ibrahim et al. 2019). A research work conducted by Jafari et al. (2016) used nanoparticle-based technique as an effective adsorbent for the removal of cadmium. The production and use of nanoparticle size activated carbon is more expensive when compared with the production and use of powdered activated carbon within the micron range.

An understanding of the nature of an activated carbon (AC) surface is required for effective and accurate interpretation of the reaction process involving AC and Cd solution. Some of the surface characteristics of interest include the net proton charge and the surface area of the AC. Uptake of Cd ions during adsorption is regulated by the surface area and surface active sites of an AC. Adsorption technique depends on several factors. These factors regulate the adsorption efficiency of a biosorbent (Ghaith et al. 2019). An understanding of the adsorption process of Cd ions onto an activated carbon surface is derived from an understanding of the reaction mechanism and reaction kinetics (Mousavi et al. 2019). Some of the parameters of interest in understanding the reaction mechanism include proton coefficient, mass transfer rate, and intraparticle diffusion. These parameters are pH and time-dependent, and a reaction model known as Freundlich isotherm is used to elucidate the proton coefficient and mass transfer rates. A Weber–Morris model is used to validate the intraparticle diffusion of Cd(II) ions onto an activated carbon surface (Abasi et al. 2019). The reaction kinetics also is regulated by contact time, the dosage of activated carbon, and initial concentration of Cd(II) in solution. An isotherm model derived by Freundlich is used to elucidate the reaction kinetics of activated carbon (AC) interaction with Cd(II) ions in solution (Park et al. 2019).

The study is aimed at using granular activated carbon (GAC) and powdered activated carbon (PAC) derived from Palmae shell to remove Cd(II) ions from aqueous media. This activated carbon from Palmae kernel shells (PKS) has been selected based on availability, low-cost, and efficient activator. An activated carbon (AC) derived from Palmae shell is a low-cost material and is widespread in the African tropics (Fuadi et al. 2014). The abundance of this palm tree

provides an opportunity for a new dimension of research in the field of biotechnology and environmental science (Lotfy et al. 2012). The objectives include the determination of the effect of contact time, initial cadmium concentration, and pH on the removal of Cd(II) ions from aqueous solution. This study was carried out at the Central Laboratory of the authors' University and Hot Laboratory in Egypt in 2018.
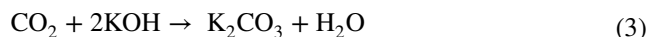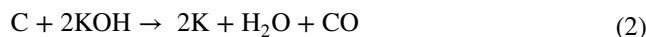
Materials and methods

Material preparation

Samples of Palmae shells were collected around local communities in Nigeria. The samples were washed with clean deionized water and air-dried at a moisture content of 10%. A pulverizer was used to produce the powdered Palmae shell. A precursor for the production of PPS (powdered Palmae shells) (i.e. some dried Palmae shells) were crushed and pulverized into less than 1 mm mesh size fraction. A mechanical crusher was used to produce the granular activated carbon. A granular Palmae (GPS) precursor was prepared by crushing some samples of the dried Palmae shells. The dried African Palmae shells were ground and segregated to granular mesh size (1–2 mm) fraction. The samples were sealed in plastic bottles ready for carbonization (Gaya et al. 2015).

Activated carbon preparation

The activation of biomass was necessary because this process increased the carbon concentration by 300%. This is since all the four components (i.e. moisture content, volatile matter content, ash content, and fixed carbon) are present after activation. Carbonization was done by pyrolysing Palmae shells to produce a large quantity of charcoal. Carbonized Palmae biomass particles were activated at a moderate temperature of 400 °C for 5 h. The activation process involved adding a solution of 75 wt% potassium hydroxide (KOH) to carbon in the ratio of 3:1 (carbon/activator) to form a paste. The content was heated until complete evaporation was achieved. A muffle furnace was used to conduct the treatment at a temperature of 400 °C in the atmosphere of neutral gas (N_2). The dried paste of the activated carbon was rinsed with distilled water at room temperature. The rinsed AC particles were further dried at 105 °C for 24 h to ensure complete drying of the particles. A reaffirmation of the particle size of the charcoal was conducted using a pulverizer and sieving to achieve 0.63 mm mesh size fraction of the powdered activated carbon (PAC). A granular activated carbon was obtained by using a mechanical crushing, followed by the sieving process to affirm a granular mesh of 1.5 mm mesh size fraction. The content was stored in sealed

plastic bottles ready for adsorption experiments (Bani et al. 2018). A set of reactions occurring during the activation process are provided as follows:

$$C + 2KOH \rightarrow 2K + H_2 + CO_2 \tag{1}$$

$$C + 2KOH \rightarrow 2K + H_2O + CO \tag{2}$$

$$CO_2 + 2KOH \rightarrow K_2CO_3 + H_2O \tag{3}$$

The formation of mesopores and micropores occurs due to intercalation of potassium into a network of carbon as activation progresses (Hui and Zaini 2015).

Characterization of biomass and activated carbon

Proximate analysis

The proximate analysis of AC was used to estimate the distribution of components of carbonized biomass. This parameter is subdivided into four groups, namely moisture content (i.e. the amount of water present in the sample), volatile matter (i.e. gases and vapours released by the sample during the heating process), fixed carbon (i.e. the carbon content of the sample), and ash (i.e. inert matter present in the sample). Moisture content was estimated by heating the sample in an oven at 105 °C for 2 h in a petri dish. The weight of the preheated and post-heated sample was measured and taken as the moisture content present in the sample. The volatile matter content was estimated by heating the sample in a muffle furnace at 925 °C in a closed crucible for 7 min. The weight of the pre-heated and post-heated sample was measured and taken as the volatile matter content present in the sample.

The ash content was determined by heating the sample in a furnace at 725 ± 25 °C in an open crucible for 1 h. The weight of the pre-heated and post-heated sample was measured and taken as the ash content present in the sample. Fixed carbon content was estimated by subtracting the % of moisture content, volatile matter content, and ash content from 100. The mathematical value represented the fixed carbon content present in the sample expressed in percentage (Budianto et al. 2019).

Ultimate analysis (CHNS)

The ultimate analysis is a method employed in the estimation of carbon, hydrogen, nitrogen, and sulphur in biomass. This technique is based on a principle derived by Dumas, which involves complete and immediate oxidation of biomass by flash combustion. Combustion results are expressed in the composition of carbon, hydrogen, nitrogen, and sulphur in percentage. The oxygen composition is calculated by

subtracting the percentages of carbon, hydrogen, nitrogen, and sulphur from 100.

The ultimate analysis was carried out in a CHNS analyser obtained from LabX, Ontario, Canada. A sample of biomass was fed into the analyser along with excess oxygen. The reaction of oxygen with other carbon, hydrogen, nitrogen, and sulphur present in the biomass releases carbon dioxide, water, nitrogen dioxide, and sulphur dioxide, respectively. These products of combustion were separated using a chromatographic column and subsequently detected by a thermal conductivity detector (TCD). This TCD provides an output signal that was proportional to the concentration of the components of the biomass (Zheng et al. 2019).

Analysis of point of zero charges of activated carbon

All chemicals and materials used for analyses were obtained from BDH (England) and Loba Chemie (India) and were of analytical grade purity. Charges exist at an AC surface. These charges are pH-dependent, and the pH at which an AC surface has a zero value is considered as a point of zero charges (pH_{pzc}). At this pH value, there is a charge boundary between positive charge surface sites and negative charge surface sites. The intrinsic surface acidity constants of AC were determined by fast potentiometric titration. 1 g of AC was added to 100 ml solution containing 0.001 M, 0.01 M, and 0.1 M of NaCl. The content was gyrated for 24 h at low speed. These samples were titrated directly with a 0.1 M NaOH. Subsequently, the pH values were read after the addition of the titrant. Three blanks samples containing 0.001 M, 0.01 M, and 0.1 M of NaCl were prepared and treated in the same manner as the preceding. The net titration curve for each ionic strength was obtained by plotting the net surface charge against the suspension pH. The curves obtained from the net titrations converge at a point that is considered as pHzpc.

Analysis of surface area of activated carbon

The specific surface area of PAC and GAC was determined by physical adsorption of nitrogen gas on the surface of the AC. The amount of nitrogen gas adsorbed equivalent to a monomolecular layer on the surface was calculated. A surface area analysis was carried out using Micromeritics (ASAP 2020) sorption analyser from LabX, Ontario, Canada. The AC was degassed at 300 °C, followed by nitrogen adsorption that was conducted at liquid nitrogen temperature of 77 K (− 196.15 °C) (Stoeckli and Centeno 2005).

Adsorption experiments

The batch equilibrium experiments were conducted by adding 2 g carbon samples to 50 ml Cd(II) solution. The mixtures were gyrated for 24 h to realize adsorption equilibrium. Subsequently, the AC was filtered using 0.45-μm membrane filters. The remaining Cd(II) concentration in solution was measured by an ICP-OES analyser (CAP6300, Thermo, USA). The adsorption capacity of the AC Qe (mg g^{-1}) was calculated using Eq. (4):

$$Q_e = [C_0 - C_e]^V/_m \tag{4}$$

where C_0 and C_e are the initial concentration and equilibrium concentration of the Cd(II) ions (mg L^{-1}), respectively, V is the volume of the solution (L), and m is the mass of AC used (g).

Cd(II) concentration between the range of 10 and 40 mg L^{-1} at $4 \leq pH \leq 8$ was equilibrated for 24 h and charged with AC at concentrations of 2–10 g L^{-1}. These concentrations and dosage were used to determine the impact of pH, dosage of AC, and initial Cd(II) concentration on the adsorption of Cd(II) ions. A mixture containing 2 g of AC charged with 10 mg L^{-1} of Cd(II) ions was made up to 50 mL. This mixture treated from 2- to 24-h period was used to determine the impact of contact time on the adsorption of Cd(II) ions by AC. Herein, this experimental set was used to deduce the mass transfer rates of the reacting system. All experiments were carried out in triplicates (i.e. to eliminate errors) at ambient temperature. A 2 g of AC was charged with 10 mg L^{-1} Cd(II) solution. Subsequently, this suspension was made up to 50 mL at $4 \leq pH \leq 8$. This mixture was used to determine the proton coefficient. The reaction mechanism was validated from the values of the proton coefficient or the proton exchange isotherm. This isotherm was deduced from the plot of the change in pH versus $\lg K_d$ as provided in Eqs. (5)–(6):

$$\alpha SOH \leftrightarrow SO^- + \alpha H^+ \tag{5}$$

$$\lg K_d \leftrightarrow \lg(K_p\{SOH\}^\alpha) + \alpha pH, \tag{6}$$

where SOH represents an AC surface reactive site, SO$^-$ is the surface-bound Cd(II), $\lg K_p$ is the apparent equilibrium binding constant, and α is the coefficient of protonation, which represents the number of protons displaced when one mole of Cd(II) binds to the AC surface (Joseph et al. 2019).

The reaction kinetics involving AC charged with Cd(II) ions was deduced from the mass transfer constant K_f. Herein, C_t/C_0 versus time provided the slopes of the curves derived from Eq. (7) Egirani et al. (2019):

$$\left[\frac{d\left(C_t/C_0\right)}{dt}\right]_{t=0} \cong -K_f S_s, \tag{7}$$

where C_0 and C_t represent the Cd(II) initial concentration and concentration at time t, S_s is the exposed surface area of an AC, and K_f is the coefficient of mass transfer. These models as derived from the Freundlich isotherm have been reviewed previously (Mohan and Chander 2001) and adopted to describe the adsorption of Cd(II) ions.

Also, the mass transfer rate and intraparticle diffusion were derived from Eqs. (8)–(9):

$$Q_t = [C_0 - C_t]^V/_m, \tag{8}$$

where C_0 is the initial Cd(II) concentration (mg L^{-1}) at time $t = 0$; C_t is the concentration (mg L^{-1}) at time t; V is the total suspension volume, and m is the mass of the AC (g) (Ojemaye et al. 2017).

An intraparticle diffusion model by Weber–Morris was also used to describe the reaction mechanism as provided in Eq. (8) (Dong 2012):

$$Q_t = K_{i0.5} + C, \tag{9}$$

where K_i is the intraparticle diffusion constant (mg g^{-1} min^{-1}) and the intercept (C) represents the effect of the layer boundary. The value of K_i is derived from the slope (K_i) of the plots of Q_t vs. $t^{0.5}$. A linear plot of Q_t versus $t^{0.5}$ indicates that intraparticle diffusion was involved in the process of adsorption (Li et al. 2016). For validation of an intraparticle diffusion, a 10 mg L^{-1} Cd(II) solution was charged with 2 g of AC made up to 50 mL at $4 \leq pH \leq 8$. This mixture was treated for 2, 4, 6, 8, 12, 18, and 24 h. Cd(II) ions remaining in solution were determined using the ICP-OES.

In all experiments, the adsorption efficiency of AC was calculated from Eq. (10):

$$\text{Adsorption efficiency (\%)} = \frac{C_0 - C_e}{C_0} \times 100, \tag{10}$$

where C_0 and C_e (mg L^{-1}) are the initial and equilibrium Cd(II) concentrations in solution, respectively (Zbair et al. 2019). In addition to the Freundlich and its derivatives used in this study, the Langmuir adsorption isotherm has been used to describe the adsorption kinetics. A linear regression is as follows: ($y = A + B \cdot x$). The Langmuir equation is represented as follows:

$$C_e/_{q_e} = \frac{1}{q_m * b} + \frac{C_e}{q_m}, \tag{11}$$

where C_e is the equilibrium concentration of cadmium (mg L^{-1}) in solution, q_e is the adsorption capacity of the activated carbon at equilibrium (mg g^{-1}), q_m is the maximum adsorption capacity of the activated carbon (mg g^{-1}), and b (L mg^{-1}) is a constant linked to the energy of adsorption. A plot of $C_e/_{q_e}$ versus C_e gives a slope of $\frac{1}{q_m}$ and an intercept $\frac{1}{q_m * b}$.

$$y = A + B * x; y = C_e/_{q_e}; x = C_e; A = \frac{1}{q_m * b}; B = \frac{1}{q_m}$$

If the adsorption process falls in line with the Langmuir model, then the plot provides a straight line and the values of q_m and b (L mg^{-1}) are evaluated from the plot.

Results and discussion

Characterization

An experimental record of proximate analysis of Palmae shell provides a distribution of its contents (Tables 1, 2, 3). The volatile matter available in Palmae shell forms a component of its contents. The moisture content present in a Palmae shell is water vapour when the temperature of the Palmae shell is raised. About 60.8% of a Palmae shell content escape from the sample following a heating process.

Table 1 Proximate analysis of powdered Palmae shell (PPS) and granular Palmae shell (GPS)

Composition	Powdered Palmae shells (PPS)	Granular Palmae shells (GPS)
Components	wt%	wt%
Moisture content	9.6	9.8
Volatile matter content	51.2	51.6
Ash content	15	14
Fixed carbon content	24.20	25.6

Table 2 Proximate and ultimate analysis of powdered Palmae shells (PPS) and granular Palmae shells (GPS)

Composition	PPS	GPS
Components	wt%	wt%
Carbon (%)	47.23	47.54
Hydrogen (%)	6.88	6.47
Nitrogen (%)	0.77	1.03
Sulphur (%)	.25	0.62
Oxygen (%)	44.86	44.33

Table 3 Proximate and ultimate analysis of powdered activated carbon (PAC) and granular Palmae activated carbon (GAC)

Composition	PAC	GAC
Components	wt%	wt%
Carbon (%)	75.00	75.26
Hydrogen (%)	1.88	2.08
Nitrogen (%)	.54	.64
Sulphur (%)	0.10	0.21
Oxygen (%)	22.48	21.81

A dramatic increase in the carbon concentration is observed on activation of the carbonized Palmae shell. This characteristic is predicated on the fact that fixed carbon is an essential component besides the volatile matter, ash content, and moisture content. This characteristic explains the dramatic fall in hydrogen content. Nitrogen found in the analysis is not a natural component of Palmae shell. Rather, this content has been introduced during the biomass pyrolysis process (i.e. during carbonization process) which is carried out under nitrogen flow condition. Nitrogen gas which is utilized during the activation process is fixed on the sample surface. A high amount of oxygen in Palmae shell is used
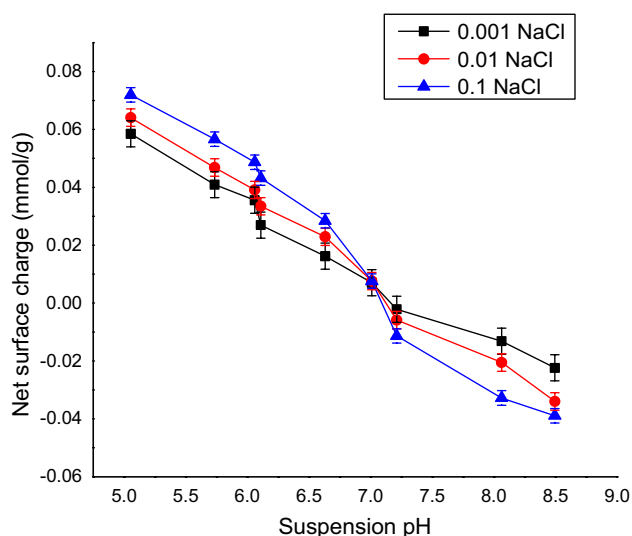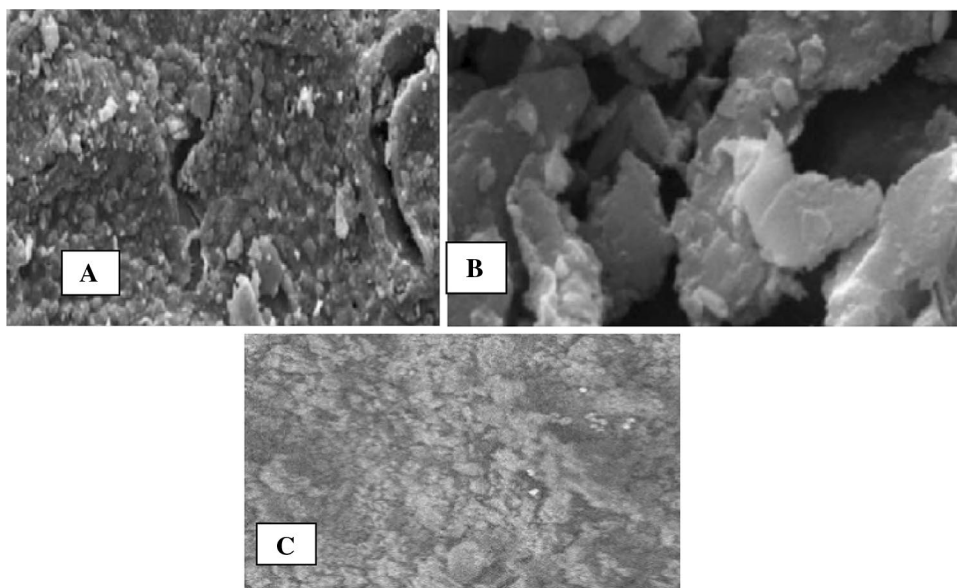
up during the activation process; thus, it is lost during the pyrolysis process.

The pH_{pzc} of activated carbon derived from potentiometric titration for both PAC and GAC was 7.01 (Fig. 1). This pH_{pzc} determined the positive and negative ions on the planar surface of a mineral. The specific surface area of the adsorbent controls the quantity of exposed mineral surface available for reaction. The surface area of PAC and GAC was calculated using the Brunauer–Emmett–Teller (BET) method. The specific surface areas per g of PAC and GAC were 2920 $m^2 g^{-1}$ and 2850 $m^2 g^{-1}$, respectively (Fig. 2).

The proton coefficient (α) was predicated on Eqs. (1) and (2), and these equations gave rise to a plot (Fig. 3), and some linear fit values (Table 4). The values of α for PAC and GAC derived from the slope were 0.28 and 0.20, respectively. This $\lg K_d$–pH plot revealed a maximum distribution coefficient (K_d) of 2.90 and 2.13 L g^{-1}, respectively. Some mass transfer constants predicated on Eq. (7) and derived from a plot of C_t/C_0 versus contact time are provided in Fig. 4 and Table 5. Some intraparticle diffusion constant was predicated on Eqs. (8) and (9) and gave rise to a plot (Fig. 5). Some slope values of these plots are provided in Table 6. This plot consists of two distinct regions, consisting of an external mass transfer and an intraparticle diffusion, respectively.

The Langmuir isotherm parameters are provided (Tables 7, 8). The Langmuir constants for PAC are higher than those of the GAC, and the maximum adsorption is equally slightly higher for the PAC compared to the GAC.

Effect of contact time on Cd(II) removal

A plot of Cd(II) removal versus contact time that was predicated on Eq. (10) provided in Fig. 6 revealed two salient
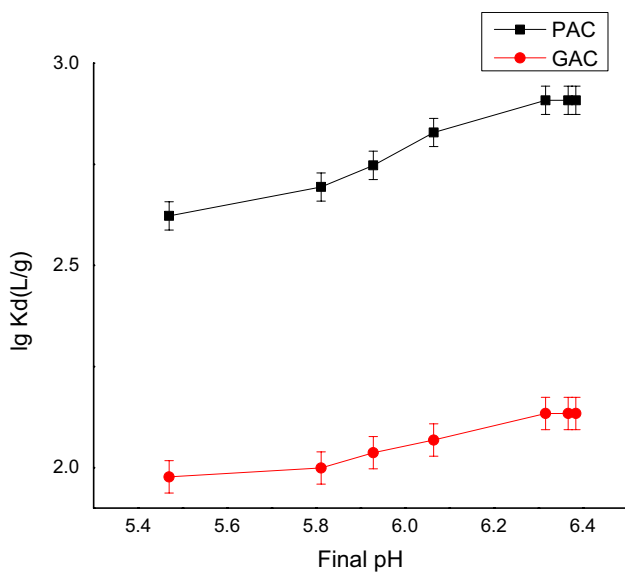

Fig. 1 Plot of net surface charge versus suspension pH of activated carbon for determination of the point of zero charges

Fig. 2 SEM micrographs of **a** Palmae shell carbon, **b** Palmae shell activated carbon, **c** Palmae shell activated carbon treated with cadmium ions

Fig. 3 Plot of $\lg K_d$ versus final pH for proton coefficient

Table 4 Linear fit parameters derived from Fig. 3

Equation	$y = a + b*x$	Value	SE
PAC			
$\lg K_d$ (L g^{-1})	Intercept	0.87	3.34^{-6}
	Slope	0.28	5.48^{-7}
GAC			
$\lg K_d$ (L g^{-1})	Intercept	0.84	2.56^{-6}
	Slope	0.20	4.24^{-7}
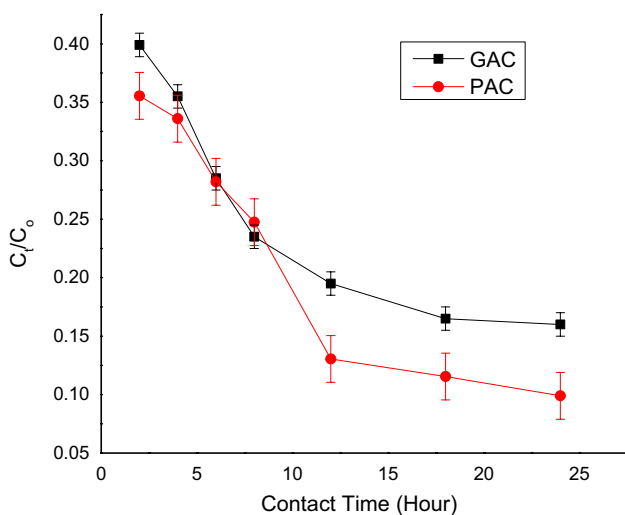
Fig. 4 C_t/C_o for cadmium adsorbed by PAC and GAC

parts for both PAC and GAC. These two parts represented the increase in adsorption as contact time was increased and steady-state adsorption for the rest of the contact period. The first part ranged from 2nd h to a 12th h. Adsorption of Cd(II) ions began to plateau at 93.2% and 83.5% at the 18th h for PAC and GAC, respectively.

Effect of initial Cd(II) concentration on Cd(II) removal

A plot of Cd(II) removal versus Cd(II) concentration in Fig. 7 revealed another two salient parts for both PAC and GAC. Cd(II) removal by both PAC and GAC decreased as Cd(II) concentration was increased. This linear trend continued from 10 mg L^{-1} to 15 mg L^{-1}. Subsequently, adsorption characterized by another phase of adsorption efficiency over the remaining range of Cd(II) concentration (20–40 mg L^{-1}) emerged. Some adsorption efficiencies of 96% and 95.85% were recorded at 10 mg L^{-1} for both PAC and GAC, respectively.

Effect of pH on Cd(II) removal

Several researchers believe that the pH stands out as the most important parameter regulating the adsorption process (Shen et al. 2019). An increase in pH above the point of zero charges (i.e. pH = 7.01) leads to a steady-state Cd(II) removal. Some maximum adsorption efficiencies of 93% and 88% were recorded at pH = 8 for both PAC and GAC, respectively.

Effect of dosage of activated carbon on cadmium removal

A plot of dosage of activated carbon versus per cent removal is provided in Fig. 8. For PAC, there was an initial linear increase in Cd(II) removal as the dosage of activated carbon was increased to 4 g. Subsequently, there was a steady nonlinear increase as the dosage of activated carbon was increased from 6 to 10 g. In the case of GAC, there was a linear increase in the removal of the Cd(II) ions as the dosage of activated carbon was increased from 4 g to 6 g. Subsequently, a steady-state Cd(II) removal emerged as activated carbon was increased. An optimum dose of activated carbon for maximum removal of the Cd(II) ions at 93% using 10 g per 50 mL of PAC, and 84.50% using 4 g per 50 mL of GAC was observed, respectively.

Discussion

Adsorption and reaction mechanism

A discussion on the reaction mechanisms is predicated on the characterization of the activated carbon. These

Table 5 Analysis of mass transfer constant derived from Fig. 4

Activated carbon type	Slope 1 (h^{-1})	Slope II (h^{-1})	Exposed surface area (cm^2)	K_{fI} ($cm^2\ h^{-1}$)	K_{fII} ($cm^2\ h^{-1}$)
PAC	8.49×10^{-2}	1.30×10^{-2}	292,000	2.91×10^{-7}	4.45×10^{-8}
GAC	9.13×10^{-2}	1.53×10^{-2}	285,000	6.67×10^{-8}	5.36×10^{-8}
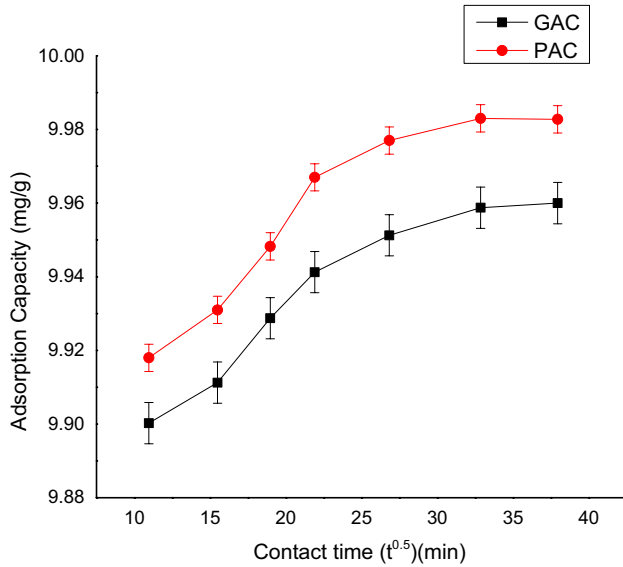
Fig. 5 A plot of adsorption capacities of PAC and GAC versus square root of contact time (min) for intraparticle diffusion

**Table 6** Linear fit analysis derived from Fig. 4 for PAC and GAC

Equation	$y = a + b*x$	Value	SE
Powdered activated carbon			
Adsorption capacity (q_m) (mg g^{-1})	Intercept	9.87	$8.09^{\wedge -7}$
	Slope	$2.57^{\wedge -3}$	$3.21^{\wedge -8}$
Granular activated carbon			
Adsorption capacity (q_m) (mg g^{-1})	Intercept	9.88	$9.20^{\wedge -7}$
	Slope	$2.93^{\wedge -3}$	$3.65^{\wedge -8}$

Table 7 Langmuir parameters for cadmium adsorbed by powdered activated carbon

pH	x	y	R^2	b (L mg^{-1})	q_m (mg g^{-1})
4	0.88	0.09	0.99	668.14	9.98
5	0.82	0.08	0.99	668.03	9.98
6	0.75	0.08	0.99	667.92	9.98
7	0.71	0.07	0.99	667.85	9.98
8	0.68	0.07	0.99	667.80	9.98
9	0.69	0.07	0.99	667.82	9.98
10	0.70	0.07	0.99	667.83	9.98

Table 8 Langmuir parameters for cadmium adsorbed by granular activated carbon

pH	x	y	R^2	b (L mg^{-1})	q_m (mg g^{-1})
4	1.38	0.138	.99	250.87	9.96
5	1.35	0.135	.99	250.85	9.96
6	1.30	0.130	.99	25	9.96
7	1.26	0.126	.99	250.79	9.96
8	1.18	0.118	.99	250.74	9.97
9	1.18	0.118	.99	250.74	9.97
10	1.18	0.118	.99	250.74	9.97
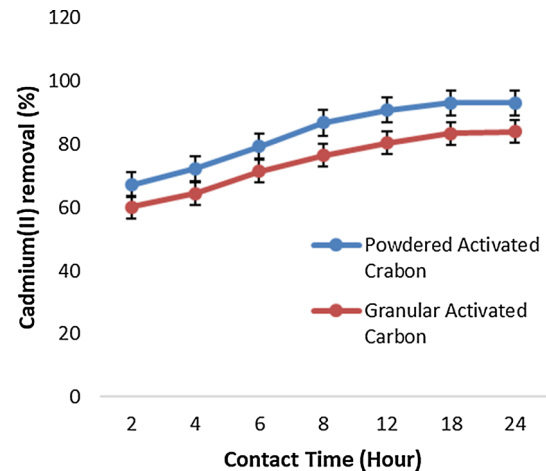
Fig. 6 Cadmium removal (%) versus contact time (hour) for powdered activated carbon (PAC) and granular activated carbon (GAC) (2 g adsorbent, pH = 5, 10 mg L^{-1} Cd(II) ions)

characteristics include proton coefficient, intraparticle diffusion, and some mass transfer rates (Ghannad and Lotfollahi 2018). Herein, the proton coefficient generated by charging Cd(II) solution with activated carbon provided values that were less than one for both PAC and GAC. These values suggested that the reaction for Cd(II) removal was not essentially controlled by protonation. The reaction with a proton coefficient greater than one implies a significant contribution of protonation in the reaction system.

The intraparticle diffusion values were slope = $2.57^{\wedge -3}$ (mg g^{-1} $min^{-0.5}$) and an intercept $C = 9.87, \neq 0$, for PAC and slope = $2.93^{\wedge -3}$ and $C = 9.88 \neq 0$ for GAC. This plot consists of two distinct regions made up of mass transfer and an intraparticle diffusion processes. These values indicated
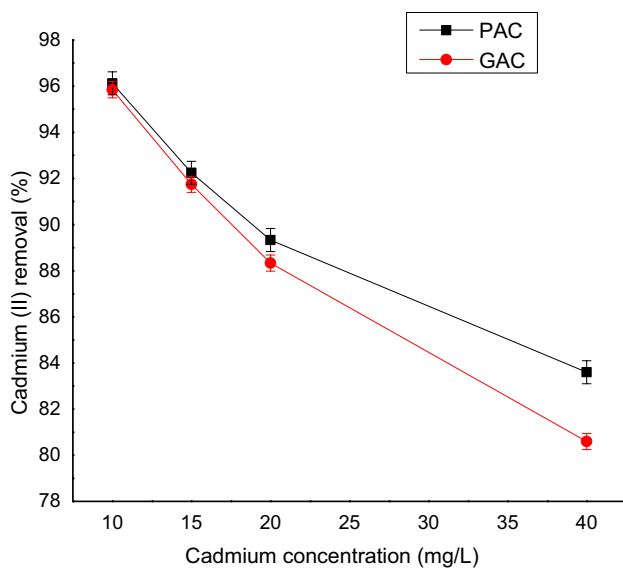
Fig. 7 Cadmium(II) removal (%) versus cadmium concentration (mg L^{-1}) for powdered activated carbon (PAC) and granular activated carbon (GAC) (2 g adsorbent, pH = 5)
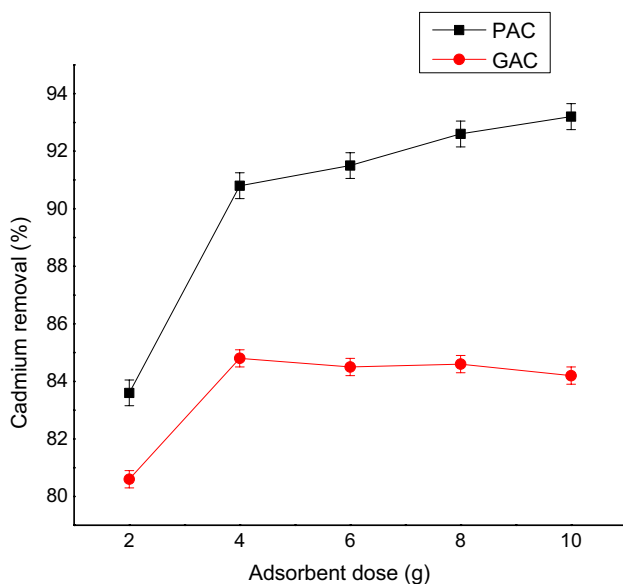

Fig. 8 Cadmium removal (%) versus dose of powdered activated carbon (PAC) and granular activated carbon (GAC) (pH = 5, 10 mg/cadmium(II) ions)

that the diffusion reaction was not a rate-limiting process and boundary layer control was involved.

Adsorption and reaction kinetics

Removal of the Cd(II) ions by activated carbon is predicated on contact time. These characteristics are derived from the plot of adsorption efficiency versus contact time

(Fig. 6). The assessment was conducted from 2 to 24 h at ambient temperature and an initial Cd(II) concentration of 10 mg L^{-1} at $4 \leq pH \leq 10$. Herein, the adsorption efficiency at pH 5 below the pH$_{pzc}$ is discussed. An increase in contact time led to an increase in adsorption efficiency. This reaction plateaued at the 12th h and became a steady-state reaction when contact time was increased.

Precipitation of heavy metal ions at this steady-state period of reaction has been suggested during adsorption (Rafatullah et al. 2011). At the onset of reaction, there were available reactive sites for Cd(II) ions to be lodged. As the reaction progresses, available reactive sites became gradually reduced and limited, thus providing a systematic saturation of these sites. Some earlier studies confirmed this trend of Cd(II) adsorption (Gour et al. 2018; Jain et al. 2018). Higher adsorption efficiency of PAC over GAC may be predicated on the higher exposed surface area of the former, thus providing more reactive sites.

In this study, the adsorption results fit into the extended Freundlich isotherm and the Langmuir isotherm derived from Eq. (11). The values of the Langmuir constant are provided in Tables 7, 8, and Fig. 9.

Adsorption process and initial Cd(II) concentration

An investigation of different initial Cd(II) concentrations is necessary because natural aqueous systems contaminated with Cd(II) ions provide a different range of concentrations. A decrease in the percentage of Cd(II) ions adsorbed is observed as the initial concentration of Cd(II) ion in solution is increased (Fig. 7) for both PAC and GAC. Surface and available reactive sites are comparatively higher for PAC than GAC. These characteristics are higher even when compared to some Cd(II) ions; thus, Cd(II) ions are retained on activated carbon at a low initial concentration of Cd(II) ions. Some Cd(II) ions are also readily adsorbed under this condition. A total sum of reactive sites is smaller than a sum of
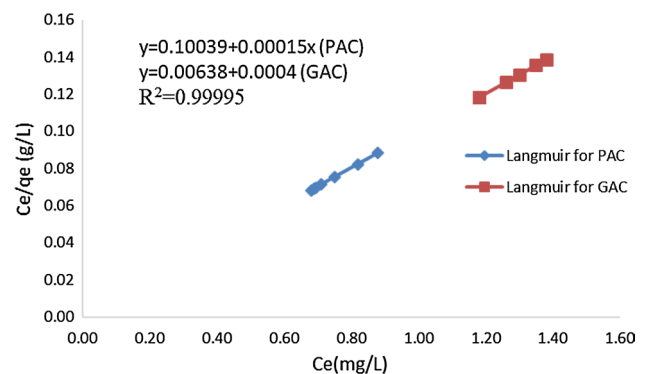

Fig. 9 Plot of C_e/q_e versus C_e for Langmuir isotherm
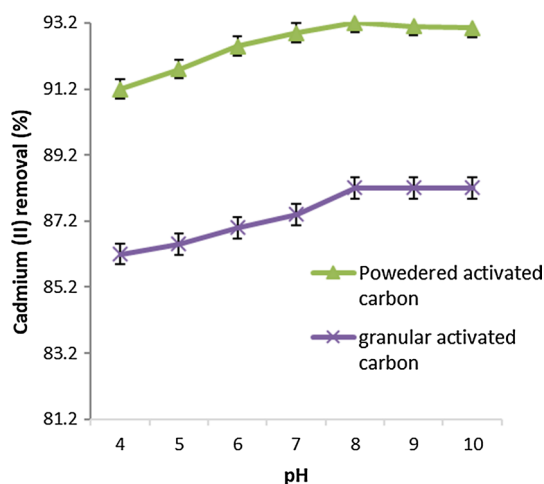
Fig. 10 Cadmium removal (%) versus pH for powdered activated carbon (PAC) and granular activated carbon (GAC) (2 g adsorbent, 10 mg L^{-1} cadmium(II) ions)

Cd(II) ions as the initial Cd(II) concentration is increased, subsequently decreasing the percentage of Cd(II) removal.

Adsorption process and pH

Herein, the pH of this mixture initiates the binding of Cd(II) ions to the surface functional group of activated carbon (Fig. 10). An increase in pH values gives rise to deprotonation of the reactive activated carbon surface, thus providing a negative charge (Burakov et al. 2018). An electrostatic attraction of a positively charged Cd(II) and negatively charged activated carbon surface in addition to hydrolysis provides a bonding. As the pH is increased to around pHzpc, a reduction in protonation and an improvement of hydroxylation are effected, thus promoting Cd(II) adsorption. These attributes lead to intraparticle diffusion and increased reorganization of the active sites of the activated carbon, thus increasing the amount of Cd(II) ions adsorbed onto activated carbon (Banerjee and Chattopadhyaya 2017). The lowering of pH gives rise to a lower percentage of adsorption. This characteristic is attributed to a competition between H_3O^+ and Cd(II) ions due to protonation of the activated carbon surface (Zheng et al. 2017).

Adsorption and dosage of activated carbon

The characteristic of doses of activated carbon charged by Cd(II) ions is represented in Fig. 8. An increase in the dose of activated carbon from 2 to 4 g provides a linear increase in adsorption of Cd(II) ions due to an increase in available reactive sites and surface area of activated carbon. Subsequently, coagulation of particles of the activated carbon sites emerged, thus providing a limited surface area and a limited reactive site. This phenomenon provides a steady state in the percentage of Cd(II) ions adsorbed. This characteristic is supported by a constant and steady-state configuration of a graphical plot provided in Fig. 8. The steady state of adsorption as a dosage of activated carbon is increased beyond 4 g which may be accounted for by the control of mass transfer rates by a concentration gradient.

Conclusion

PAC and GAC were successfully prepared as novel biosorbents. The physical and chemical characteristics of the activated carbon were characterized using standard laboratory procedures. A batch mode adsorption system was used to test the adsorption of Cd(II) by PAC and GAC. The mechanism of the reaction characteristics involved in adsorption of Cd(II) ions is predicated on the activities of a proton coefficient that was less than one, mass transfer rates that indicated a two-reaction process, and an intraparticle diffusion that was controlled by the boundary layer.

The adsorption efficiency recorded an initial increase, followed by a steady-state characteristic for all parametric plots but initial Cd(II) concentration. These characteristics suggest that the active and reactive sites at activated carbon surface become gradually saturated as the adsorption process progresses. A pattern of adsorption essentially regulated by hydrolysis increased the reorganization of reactive sites, and reactive support of activated carbon surface has emerged.

Compliance with ethical standards

Conflict of interest No potential conflict of interest was reported by the authors.

References

Abasi CY, Ejidike IP, Dikio ED (2019) Synthesis, characterisation of ternary layered double hydroxides (LDH) for sorption kinetics and thermodynamics of Cd^{2+}. Int J Environ Stud 76(3):441–455

Banerjee S, Chattopadhyaya M (2017) Adsorption characteristics for the removal of a toxic dye, tartrazine from aqueous solutions by a low cost agricultural by-product. Arab J Chem 10:S1629–S1638

Bani O, Aryani N, Kaban GS (2018) Preparation of activated carbon-based catalyst from candlenut shell impregnated with KOH for biodiesel production. Key Eng Mater 777:262–267

Barsbay M, Kavaklı PA, Tilki S, Kavaklı C, Güven O (2018) Porous cellulosic adsorbent for the removal of Cd(II), Pb(II) and Cu(II) ions from aqueous media. Radiat Phys Chem 142:70–76

Budianto A, Kusdarini E, Effendi S, Aziz M (2019) The production of activated carbon from Indonesian mangrove charcoal. In: IOP conference series: materials science and engineering. IOP Publishing, p 012006

Burakov AE et al (2018) Adsorption of heavy metals on conventional and nanostructured materials for wastewater treatment purposes: a review. Ecotoxicol Environ Saf 148:702–712

Di Stasi C, Alvira D, Greco G, González B, Manyà JJ (2019) Physically activated wheat straw-derived biochar for biomass pyrolysis vapors upgrading with high resistance against coke deactivation. Fuel 255:115807

Dong H (2012) Clay–microbe interactions and implications for environmental mitigation. Elements 8(2):113–118

Egirani DE, Poyi NR, Wessey N (2019) Synthesis of zinc oxide–montmorillonite composite and its effect on the removal of aqueous lead ions. Acta Geochim 38(1):120–130

Fuadi NA, Ibrahem AS, Ismail KN (2014) Removal of heavy metals from simulated wastewater using physically and chemically modified palm shell activated carbon. J Appl Sci 14(12):1294

Gaya UI, Otene E, Abdullah AH (2015) Adsorption of aqueous Cd(II) and Pb(II) on activated carbon nanopores prepared by chemical activation of doum palm shell. SpringerPlus 4(1):458

Ghaith E, Rizvi S, Namasivayam C, Rahman P (2019) Removal of Cd^{++} from contaminated water using bio-surfactant modified ground grass as a bio-sorbent. In: 2019 advances in science and engineering technology international conferences (ASET). IEEE, pp 1–7

Ghannad SS, Lotfollahi MN (2019) Preparation of granular composite materials as novel sorbents and their application for removal of heavy metals from solution. Int J Environ Sci Technol 16(7):3697–3706

Gour K, Donadkar DK, Rahangdale PK (2018) Adsorptive removal of CD (II) using activated carbon prepared from bark of ficusracemosa. IOP Conf Ser: Mater Sci Eng 410(1):012013

Hui TS, Zaini MAA (2015) Potassium hydroxide activation of activated carbon: a commentary. Carbon Lett 16(4):275–280

Imran M et al (2019) Kinetic and equilibrium studies for cadmium biosorption from contaminated water using *Cassia fistula* biomass. Int J Environ Sci Technol 16(7):3099–3108

Jafari KA, Baghdadi M, Pardakhti A (2016) Removal of cadmium and lead from aqueous solutions by magnetic acid-treated activated carbon nanocomposite. Desalin Water Treat 57(40):18782–18798

Jain M, Yadav M, Kohout T, Lahtinen M, Garg VK, Sillanpää M (2018) Development of iron oxide/activated carbon nanoparticle composite for the removal of Cr (VI), Cu (II) and Cd (II) ions from aqueous solution. Water Resour Indus 20:54–74

Janković B et al (2019) Physico-chemical characterization of carbonized apricot kernel shell as precursor for activated carbon preparation in clean technology utilization. J Clean Prod 236:117614

Joseph L, Jun BM, Flora JR, Park CM, Yoon Y (2019) Removal of heavy metals from water sources in the developing world using low-cost materials: a review. Chemosphere 229:142–159

Li H, Ye X, Geng Z, Zhou H, Guo X, Zhang Y, Zhao H, Wang G (2016) The influence of biochar type on long-term stabilization for Cd and Cu in contaminated paddy soils. J Hazard Mater 304:40–48

Lotfy HR, Misihairabgwi J, Mutwa MM (2012) The preparation of activated carbon from agroforestry waste for wastewater treatment. Afr J Pure Appl Chem 6(11):149–156

Mohan D, Chander S (2001) Single component and multi-component adsorption of metal ions by activated carbons. Colloids Surf A 177(2–3):183–196

Mousavi SA, Pirsaheb M, Faraji M (2019) Cadmium(II) removal from aqueous solution by activated carbon of India shrub wood: optimization, equilibrium and kinetic modeling. Desalin And Water Treat 145:160–168

Ojemaye MO, Okoh OO, Okoh AI (2017) Surface modified magnetic nanoparticles as efficient adsorbents for heavy metal removal from wastewater: progress and prospects. Mater Express 7(6):439–456

Park JH, Wang JJ, Kim Seong-Heon Kang S-W, Jeong CY, Jeon J-R, Park KH, Cho J-S, Delaune RD, Seo D-C (2019) Cadmium adsorption characteristics of biochars derived using various pine tree residues and pyrolysis temperatures. J Colloid Interface Sci 553:298–307

Rafatullah M, Sulaiman O, Hashim R, Amini MH (2011) Adsorption of copper (II) ions onto surfactant-modified oil palm leaf powder. J Disper Sci Technol 32(11):1641–1648

Sadegh H, Mazloumbilandi M, Chahardouri M (2017) Low-cost materials with adsorption performance. In: Martínez L, Kharissova O, Kharisov B (eds) Handbook of ecomaterials. Springer, Cham, pp 1–33

Šapčanin A, Smajović A, Pehlić E, Salihović M, Jančan G (2019) Health risk assessments based on the contents of heavy metals in Sarajevo urban soil. In: International conference "new technologies, development and applications". Springer, pp 595–603

Shen Z, Fan X, Hou D, Jin F, O'Connor D, Tsang DC, Ok YS, Alessi DS (2019) Risk evaluation of biochars produced from Cd-contaminated rice straw and optimization of its production for Cd removal. Chemosphere 233:149–156

Shahraki ZH, Sharififard H, Lashanizadegan A (2018) Grape stalks biomass as raw material for activated carbon production: synthesis, characterization and adsorption ability. Mater Res Express 5(5):055603

Sierra-Marquez L, Espinosa-Araujo J, Atencio-Garcia V, Olivero-Verbel J (2019) Effects of cadmium exposure on sperm and larvae of the neotropical fish Prochilodus magdalenae. Comp Biochem Physiol C: Toxicol Pharmacol 225:108577

Stoeckli F, Centeno TA (2005) On the determination of surface areas in activated carbons. Carbon 43(6):1184–1190

Thambiliyagodage C, Cooray V, Perera I, Wijesekera R (2018) Eco-friendly porous carbon materials for wastewater treatment.

In: International conference on sustainable built environment. Springer, pp 252–260

Wan Ibrahim WMH, Mohamad Amini MH, Sulaiman NS, Kadir WRA (2019) Powdered activated carbon prepared from *Leucaena leucocephala* biomass for cadmium removal in water purification process. Arab J Basic Appl Sci 26(1):30–40

Wang F, Yang W, Cheng P, Zhang S, Zhang S, Jiao W, Sun Y (2019) Adsorption characteristics of cadmium onto microplastics from aqueous solutions. Chemosphere 35:1073–1080

Yacob AR, Hanapi SZ, Inderan V, Dasril RS (2010) Nano-tungsten carbide prepared from palm kernel shell for catalytic decomposition of hydrazine. Chem Biol Environ Eng. https://doi.org/10.1142/9789814295048_0067

Yang X, Zhao C, Xu J, Zhang J, Guo Z, Shao Y (2019) Surface functional groups of carbon-based adsorbents and their roles in the removal of heavy metals from aqueous solutions: a critical review. Chem Eng J 366:608–621

Yin W, Zhao C, Xu J, Zhang J, Guo Z, Shao Y (2019) Removal of Cd (II) and Ni (II) from aqueous solutions using activated carbon developed from powder-hydrolyzed-feathers and Trapa natans husks. Colloids Surf A Physicochem Eng Asp 5(560):426–433

Zbair M, Ahsaine HA, Anfar Z, Slassi A (2019) Carbon microspheres derived from walnut shell: rapid and remarkable uptake of heavy metal ions, molecular computational study and surface modeling. Chemosphere 231:140–150

Zhang H, Reynolds M (2019) Cadmium exposure in living organisms: a short review. Sci Total Environ 678:761–767

Zheng M, Hu Q, Zhang S, Tang H, Li L, Pang H (2017) Macroporous activated carbon derived from rapeseed shell for lithium–sulfur batteries. Appl Sci 7(10):1036

Zheng C, Ma X, Yao Z, Chen X (2019) The properties and combustion behaviors of hydrochars derived from co-hydrothermal carbonization of sewage sludge and food waste. Biores Technol 285:121347